Sound Field Control With Hemi-Cylindrical Loudspeaker Arrays

Falk-Martin Hoffmann, Filippo Maria Fazi, Simone Fontana

14. July, 2016

Abstract

An acoustical model for the sound field generated by hemi-cylindrical loudspeaker arrays is presented and a method for beamforming is derived. The sound field model is obtained by introducing two independent boundary conditions for the sound field of a single impinging plane wave. The model for the radiation from a single loudspeaker in the array is then obtained from the reciprocity principle. Various beam patterns are presented and evaluated as to their dependency on frequency. The obtained theoretical results are discussed, along with a plan for future experimental work.

1 Introduction

Unlike the widely spread microphone arrays, which can already be found in various applications in our every day life, loudspeaker arrays still represent a niche technology. They are typically used in large scale public address systems (e.g. for music concerts) and lately also in the form of sound bars as an extension to the TV sound system. In either case, they typically seek to provide the user with sound field control based on beamforming. Circular or spherical loudspeaker arrays that seek to synthesise a sound field within a bounded area [1, 2, 3] still remain experimental applications. These type of installations often require very large numbers of loudspeakers and acoustical treatment of the room to perform at their optimum. This may be the reason why they have been so far less appealing for consumer products.

As with most sound field control applications, the more accurate the sound field model, the better the system performance. A typical assumption made in the design theory of linear or circular arrays on rigid baffles is that they are used in perfect free field conditions [2, 4, 5]. For most installations this assumption is already invalid from the start, typically due to the presence of a floor, a ceiling or any other obstructions to propagating waves that are not included in the model. In other words,

every obstruction that is included in the acoustic model makes the system more suitable for every day applications.

Kolundzija et al. presented an initial prototype for cylindrical loudspeaker arrays for beamforming applications in the full audible band [6, 7]. Betlehem and Poletti proposed to apply cylindrical loudspeaker arrays in reverberant environments to increase the degree of sound field control by using reflective walls to deploy secondary sources [8, 9, 10]. Fazi et al. proposed a strategy for beamforming with circular loudspeaker arrays installed on rigid cylindrical baffles by using Neumann Green Functions to model the sound field contribution of the individual speakers [11, 12].

This work extends the theory presented by Fazi et al. [11, 12] to model the radiated sound field of *hemi-circular arrays* installed on a rigid hemi-cylinder arranged on an infinite planar rigid baffle. A mathematical model of the acoustic radiation of such arrays is provided along with a number of simulated fields. The unique properties of these types of arrays are discussed on the basis of the model and the simulated data.

The remainder of this work is organised as follows: The second section introduces the acoustic model and derives the far field radiation solution for the proposed array design. In the third section, the inverse solution to the radiation problem is derived in order to obtain the loudspeaker driving functions for a desired beam pattern. The fourth section focuses on the system's radial functions and their influence on the array's low frequency performance. The overall beamforming performance is then investigated theoretically on the basis of the developed model. The results are discussed in the penultimate section and summarised in the last section with an outlook on further work.

2 Acoustic Model

The coordinate system used in this work is shown in Figure 1. In the course of this section, the considered propagation space is modelled by introducing two boundary conditions to the general free field model in order to suit the intended scenario.

In accordance with the work presented in [11], each speaker in the system is approximated by assuming a point source on a rigid baffle with a given acoustic strength q_l. The mathematical concept for the field radiated from such sources is known as the Neumann Green Function (NGF) G_N [13]. The function arguments of the NGF comprise the evaluation point and the location of the point source, as well as (often implicitly) the frequency ω. Combining the NGFs for L loudspeakers in a hemi-cylindrical

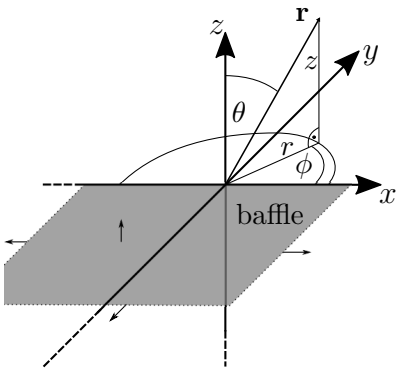

Figure 1: General coordinate system for the mathematical model.

array yields the sound field model given by

$$p(r, \phi, z, \omega) = \sum_{l=1}^{L} G_{\mathrm{N}}(R, \phi_l, z_l, r, \phi, z, \omega) q_l(\omega). \tag{1}$$

Note that R is the radius of both, the hemi-cylindrical baffle and the arc on which the loudspeakers are arranged.

Equation (1) describes the forward problem for the type of array under consideration. The main difference between the model of a speaker on a full cylinder to that of a loudspeaker on a hemi-cylinder attached to an infinite planar baffle is that its radiated sound field is reflected from the baffle behind the cylinder. A reflection from a point source is however not a novel concept and can be easily factored in by assuming a mirror source behind the baffle [14]. The concept is depicted in Figure 2 and states

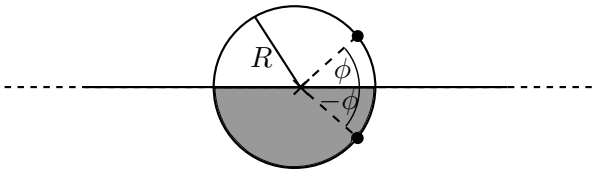

Figure 2: Model of the point source on a rigid baffle (upper half) with radius R located at the angle ϕ and a mirror source on a baffle (lower half) on the other side of the wall located at $-\phi$.

that every point source located at $\mathbf{r} = (R, \phi, z)^T$ has a mirror source located at $\mathbf{r} = (R, -\phi, z)^T$. Since both the original source and the mirror source are point sources, their individual sound fields can be calculated from the NGF for cylindrical arrays. However, one objective of this paper is to present a NGF for hemicylindrical arrays that incorporates both sources in one. Its derivation is shown in the following subsection.

2.1 The Neumann Green Function

The Neumann Green function is derived in several steps, starting from a general expression for the pressure field. This model is then amended to incorporate the scattering from an infinite hemi-cylinder on a planar baffle. The far field approximation of the Neumann Green function is then obtained from the pressure on the surface of the hemi-cylinder due to an impinging plane wave through reciprocity.

2.1.1 General Sound Field Expansion

The general model for a sound field in cylindrical coordinates that is valid in $\mathbb{R}^3$ for a given angular frequency ω is given in terms of a set of coefficients $\{C_n(k_z)\}_{n\in\mathbb{Z}}$ by the series expansion

$$p_{\mathrm{FS}}(r,\phi,z) = \sum_{n=-\infty}^{\infty} \frac{e^{in\phi}}{\sqrt{2\pi}} \int_{-\infty}^{\infty} \frac{e^{ik_z z}}{\sqrt{2\pi}} J_n(k_r r) C_n(k_z) dk_z, \tag{2}$$

with $k = \sqrt{k_z^2 + k_r^2}$, where k is the acoustic wave number, k_z the axial and k_r the radial component, respectively. $J_n(x)$ is the Bessel function of the nth order [13]. The dependency of ω is omitted for the sake of brevity.

The next step on the way to an NGF for hemi-cylindrical arrangements is to limit the propagation space by setting appropriate boundary conditions.

2.1.2 The Infinite Planar Baffle

Introducing a rigid infinite baffle in the x-z-plane is equivalent to imposing the boundary condition

$$\frac{\partial p(r,\phi,z)}{\partial \phi}|_{\phi=0,\pi} = 0 \tag{3}$$

for the pressure gradient. This effectively limits the propagation space to $V := \{r,\phi,z : r \in \mathbb{R}^+ \cup 0, 0 \leq \phi \leq \pi, z \in \mathbb{R}\}$ (see Figure 1). The mirror source model inherently enforces the above boundary condition. Therefore, by mirroring the existing pressure field p w.r.t. the boundary plane $\phi = 0, \pi$, one yields the image p_{M} to the original field. Due to the nature of the angular basis functions $\frac{e^{in\phi}}{\sqrt{2\pi}}$, the image of p is given through the complex conjugation of the former, yielding

$$p_{\mathrm{M}}(r,\phi,z) = \sum_{n=-\infty}^{\infty} \frac{e^{-in\phi}}{\sqrt{2\pi}} \int_{-\infty}^{\infty} \frac{e^{ik_z z}}{\sqrt{2\pi}} J_n(k_r r) C_n(k_z) dk_z. \tag{4}$$

The sum of p and p_{M} yields the pressure field of a point source in the half space

$$\begin{aligned} & p_{\mathrm{HS}}(r,\phi,z) \\ & = \sum_{n=-\infty}^{\infty} \frac{e^{in\phi}+e^{-in\phi}}{\sqrt{2\pi}} \int_{-\infty}^{\infty} \frac{e^{ik_z z}}{\sqrt{2\pi}} J_n(k_r r) C_n(k_z) dk_z \\ & = \sum_{n=-\infty}^{\infty} \frac{2\cos(n\phi)}{\sqrt{2\pi}} \int_{-\infty}^{\infty} \frac{e^{ik_z z}}{\sqrt{2\pi}} J_n(k_r r) C_n(k_z) dk_z. \end{aligned} \tag{5}$$

With the angular basis functions reduced to $\cos(n\phi)$, it can be seen that the pressure field p_{HS} now satisfies the boundary condition (3). Using the Bessel function relation $J_{-n}(x) = (-1)^n J_n(x)$ [13], the expression for p_{HS} can be further simplified to

$$\begin{aligned} & p_{\mathrm{HS}}(r,\phi,z) = \\ & \sum_{n=0}^{\infty} \nu_n \frac{\cos(n\phi)}{\sqrt{2\pi}} \int_{-\infty}^{\infty} \frac{e^{ik_z z}}{\sqrt{2\pi}} J_n(k_r r) D_n(k_z) dk_z, \end{aligned} \tag{6}$$

with

$$D_n(k_z) = \nu_n \left[C_n(k_z) + (-1)^n C_{-n}(k_z) \right], \tag{7}$$

$$\nu_n = \sqrt{2 - \delta_n}, \tag{8}$$

where δ_n denotes the Kronecker Delta [15].

Equation (6) serves as an analytical model for sound propagation in the half-space. In the next step, the scattering from an infinite rigid hemi-cylinder is added to the model.

2.1.3 Scattering from Infinite Hemi-Cylinder

A full derivation of the scattering from a rigid object at the origin of a coordinate system can be found in the literature, e.g. [13]. The main concept is to find a scattered pressure field p_{S} complementing an incident pressure field p_I that satisfies the Neumann boundary condition

$$\frac{\partial p_{\mathrm{S}}(r,\phi,z)}{\partial r} + \frac{\partial p_{\mathrm{I}}(r,\phi,z)}{\partial r} = 0 \tag{9}$$

on the scatterer's surface S. For an infinite hemi-cylindrical scatterer, its surface is given by $S = \{r,\phi,z : r = R, 0 \leq\leq \pi, z \in \mathbb{R}\}$. Following a similar derivation to that presented in [13], the total field

for $r \geq R$ is obtained as

$$\begin{aligned} & p(r, \phi, z) \\ & = \sum_{n=0}^{\infty} \nu_n \frac{\cos(n\phi)}{\sqrt{2\pi}} \int_{-\infty}^{\infty} \frac{e^{ik_z z}}{\sqrt{2\pi}} R_n(k_r, r, R) D_n(k_z) dk_z, \end{aligned} \tag{10}$$

with

$$R_n(k_r, r, R) = J_n(k_r r) - \frac{J_n'(k_r R)}{H_n^{(1)\prime}(k_r R)} H_n^{(1)}(k_r r), \tag{11}$$

where $H_n^{(1)}(x)$ denotes the Hankel function of the first kind and the superscript $'$ indicates the derivative of the Bessel and Hankel function, respectively [13].

The sound field model for the half space with a rigid infinite hemi-cylinder around the origin is now fully defined by eq. (10). The NGF can then be found from the reciprocity principle. By calculating the pressure caused by an incoming single plane wave at a point (R, ϕ_l, z_l) on the surface of the hemi-cylinder, it is possible to model the *far field radiation* in the direction of the impinging plane wave from a point source located at the same point.

The next subsection introduces the plane wave expansion for the restricted propagation space with a hemi-cylindrical scatterer at the origin.

2.1.4 Field of an Impinging Plane Wave

For a single plane wave impinging from (ϕ_q, θ_q), the sound field coefficients C_n of the general model in (2) are given through the Jacobi-Anger Expansion [16] and an additional axial component [13], so that

$$C_n(k_z) = \sqrt{2\pi}\delta(k_z - k\cos\theta_q) i^{-n} \frac{e^{-in\phi_q}}{\sqrt{2\pi}}. \tag{12}$$

Using eqs. (7) and (12), the coefficients for the model of a plane wave impinging into the half space are given as

$$\begin{aligned} & D_n(k_z) \\ & = \nu_n \sqrt{2\pi}\delta(k_z - k\cos\theta_q) \left[i^{-n} \frac{e^{-in\phi_q}}{\sqrt{2\pi}} + (-1)^n i^n \frac{e^{in\phi_q}}{\sqrt{2\pi}} \right] \\ & = \nu_n \sqrt{2\pi}\delta(k_z - k\cos\theta_q) i^{-n} 2 \frac{\cos(n\phi_q)}{\sqrt{2\pi}}. \end{aligned} \tag{13}$$

Using equation (13) in (10) yields the pressure for a plane wave propagating in the half-space and impinging on a hemi-cylindrical scatterer at the origin

$$\begin{aligned} & p(r,\phi,z) \\ & = e^{ik\cos\theta_q z}\sum_{n=0}^{\infty}\nu_n^2 i^{-n}2\frac{\cos(n\phi_q)}{\sqrt{2\pi}}\frac{\cos(n\phi)}{\sqrt{2\pi}}R_n(k_r,r,R), \end{aligned} \tag{14}$$

where $k_r = k\sin\theta_q$.

2.1.5 Far Field Neumann Green Function

The result in (14) can be further simplified for the case that $(r,\phi,z)\in S$ by exploiting the Wronskian relation [13]

$$H_n^{(1)\prime}(\xi)J_n(\xi) - J_n'(\xi)H_n^{(1)}(\xi) = \frac{i2}{\pi\xi}, \tag{15}$$

resulting in the far field expression for the Neumann Green function

$$\begin{aligned} & G_{\mathrm{N}}(R,\phi_l,z_l,\theta_q,\phi_q,\omega) = \\ & \quad e^{ik\cos\theta_q z_l}\sum_{n=0}^{\infty} i^{-n}\nu_n^2\frac{i2\cos(n\phi_l)\cos(n\phi_q)}{\pi^2 kR\sin(\theta_q)H_n'(kR\sin\theta_q)}. \end{aligned} \tag{16}$$

Equation (16) models the far field radiation of a point source. For frequencies whose wavelength is large in comparison to the diaphragm, a loudspeaker can be approximated as a point source (monopole) [17].

The far field radiation of an array with L loudspeakers can then be modelled in the x-y-plane (i.e. $z=0$ and $\theta_q = \frac{\pi}{2}$) by the sum of the solution in (16) for the different speaker locations ϕ_l, so that the far field pressure

$$\begin{aligned} p(\phi,\omega,q_l) &= \sum_{l=1}^{L} G_{\mathrm{N}}(R,\phi_l,0,\frac{\pi}{2},\phi,\omega)q_l(\omega) \\ &= \sum_{l=1}^{L}\sum_{n=0}^{\infty}\nu_n^2\cos(n\phi_l)\cos(n\phi)b_n(kR)q_l(\omega), \end{aligned} \tag{17}$$

is given as a function of the driving functions $q_l(\omega)$ with

$$b_n(\xi) = \frac{i2}{i^n\pi^2 kRH_n'(\xi)}. \tag{18}$$

Equation (17) describes a forward problem of the far field pressure resulting from a given set of $q_l(\omega)$. To find the set of $q_l(\omega)$ that yield a desired radiation pattern

$$f(\phi,\omega) = \sum_{n=0}^{\infty} \nu_n \cos(n\phi) f_n(\omega) \tag{19}$$

in the far field requires solving the corresponding inverse problem [16]. A method to obtain the solution to the latter is described in the next section.

3 Loudspeaker Driving Functions

The L drivers of the array are assumed to be regularly distributed along the intersection of S with the x-y-plane and located at the angles

$$\phi_l = (l - \frac{1}{2})\frac{\pi}{L}, l = 1 \dots L. \tag{20}$$

Then, without loss of generality, the L driving functions $q_l(\omega)$ can be described through L coefficients $q_{n'}(\omega)$ as an expansion of the orthogonal set of basis functions [18] $\{\nu_n \cos(n\phi)\}_{n=0}^{N}$, so that

$$q_l(\omega) = \sum_{n'=0}^{N} \nu_{n'} \cos(n'\phi_l) q_{n'}(\omega),\ N = L - 1. \tag{21}$$

Equation (21) poses a fully determined system of linear equations. The set of coefficients $\{q_{n'}(\omega)\}_{n'=0}^{N}$ can be related to the coefficients $f_n(\omega)$ of a desired radiation pattern by comparing (17) and (19), finding that

$$\sum_{l=1}^{L} \nu_n \cos(n\phi_l) b_n(kR) q_l(\omega) = f_n(\omega). \tag{22}$$

Replacing $q_l(\omega)$ in (22) by the result in (21) yields

$$f_n(\omega) = \\ b_n(kR) \sum_{n'=0}^{N} q_{n'}(\omega) \sum_{l=1}^{L} \nu_n \cos(n\phi_l) \nu_{n'} \cos(n'\phi_l). \tag{23}$$

For the given definition of ϕ_l, the above equation can be further simplified by exploiting the orthogonality relation [16, 13]

$$\sum_{l=1}^{L} \nu_n \cos(n\phi_l)\nu_{n'} \cos(n'\phi_l) = L\delta_{n-n'},\ n, n' < L, \tag{24}$$

yielding

$$f_n(\omega) = Lb_n(kR)q_n(\omega) = \Gamma_n(kR)q_n(\omega) \tag{25}$$

for $n \leq N$. The *radial functions* for the far field radiation model are denoted as $\Gamma_n(kR)$. The limitation w.r.t. n is due to the finite number of drivers. For an infinite number of point sources in the array, the sum in (24) becomes an integral, making it valid for $n, n' \in \mathbb{N}_0$.

Rewriting equation (25) for $q_n(\omega)$ and applying the result in (21) for $n' = n$ yields the result for the calculation of the driving functions:

$$q_l(\omega) = \sum_{n=0}^{N} \nu_n \cos(n\phi_l) \frac{1}{\Gamma_n(kR)} f_n(\omega), l = 1 \ldots L. \tag{26}$$

As a consequence of (24), an array with L drivers can only control radiation patterns $f(\phi, \omega)$ of the form in (19) that are limited w.r.t. their highest order to $N = L - 1$, so that $f_n(\omega) = 0$ for $n > N$.

Lacking control of higher orders does not, however, mean that the orders excited by the array are inherently limited to N as well (compare the expression in (17)). Orders $n_a \geq L$ are the reason for spatial aliasing [3], provided that they radiate into the far field. Whether an order n radiates to the far field for a specific frequency f or not depends on the radial functions $\Gamma_n(kR)$, which are investigated in more detail in the next section.

4 Radial Functions $\Gamma_n(kR)$

The importance of radial functions is mutual to both circular and spherical transducer array analysis [19, 2, 20] because they determine the modes' radiation behaviour. The radial functions $\Gamma_n(kR)$ for the orders $n = 0 \ldots 6$ are given in Fig. 3 for an array with $R = 0.15$ m. As with most arrays based on a model in spherical or cylindrical coordinates, the low frequencies are mainly dominated by the lower orders, while towards high frequencies all considered modes eventually radiate with roughly the same magnitude. The latter statement entails that spatial aliasing is bound to occur at high frequencies. Nevertheless, the number of orders n that contribute to spatial aliasing within the audible band is

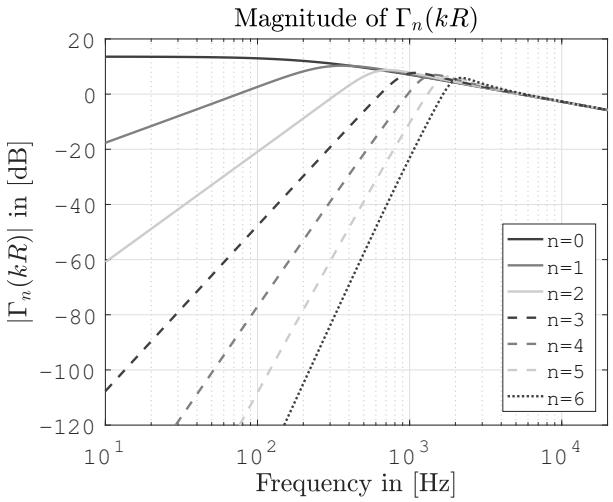

Figure 3: Development of $\Gamma_n(kR)$ over the audible spectrum for $R = 0.15$ m.

limited due to evansecent behaviour of modes higher than a system-specific bound $n = n_A$ [13, 21].

While aliasing remains a high frequency problem, sound field control at low frequencies is prone to be affected by ill-conditioning [22]. With $\Gamma_n(kR)$ dropping significantly in magnitude at low frequencies as the order increases, the solution for $q_l(\omega)$ in (26) may require a diaphragm displacement that is beyond the dynamic capacities of the driver [12]. Therefore a regularisation factor β needs to be introduced that ensures the stability of the system. The regularised driving functions are then given by

$$q_l(\omega) = \sum_{n=0}^{N} \nu_n \cos(n\phi_l) \frac{\Gamma_n(kR)^*}{|\Gamma_n(kR)|^2 + \beta\sigma^2} f_n(\omega) \tag{27}$$

with

$$\sigma = \max |\Gamma_n(kR)|. \tag{28}$$

Effectively, this normalised Tikhonov regularisation limits the degree of sound field control at lower frequencies but improves the robustness of the system [12].

5 Beamforming Performance

The target beam patterns used in this work are given as

$$f(\phi) = \sum_{n=0}^{N'} \frac{\nu_n \cos(n\phi_B)}{\sum_{n=0}^{N'} \nu_n^2 \cos(n\phi_B)^2} \nu_n \cos(n\phi). \tag{29}$$

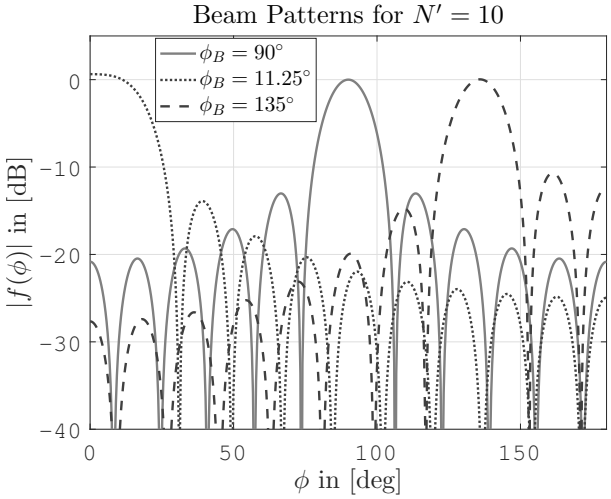

Figure 4: Theoretical beam patterns for three different angles ϕ_B with $N' = 10$.

for a beam in direction ϕ_B. Unlike with circular arrays on full cylinders, the exact beam pattern of hemicylindrical arrays depends on the steering direction of the beam, as can be understood from Fig. 4. This effect occurs due to the lack of direction-independent symmetry in combination with the cosine nature of the basis functions: a fully symmetric sound field is obtained only with a beam directed at $\phi_B = \frac{\pi}{2}$, while for every other ϕ_B, the main lobe will be closer to one side of the planar baffle behind the hemi-cylinder.

The normalisation by $\sum_{n=0}^{N'} \nu_n^2 \cos(n\phi_B)^2$ in (29) is required to ensure that the magnitude of the beam in the designated direction is unity. However, note that for $\phi_B = 11.25°$it can be observed that the maximum of the beam pattern is *not* at ϕ_B. This phenomenon occurs towards the angular limits of the propagation space, yet a deeper insight into this problem lies beyond the scope of this work.

The findings above are also reflected in the simulated beam patterns depicted in Figure 5. These were calculated on the basis of the driving functions in (27) with $\beta = 0.1$. It can be seen that the side lobes for an array with $R = 0.15$ m and $L = 15$ speakers are theoretically approx. 12 dB below the level of the main lobe within the optimal frequency band [12]. The optimal band can be deduced from the results in Figure 5 as 3 kHz $< f_{\text{opt}} <$ 6 kHz. For frequencies lower than 3 kHz the array shows the effect of the regularisation where the beam becomes wider as frequency decreases. For frequencies beyond 6 kHz the effects of spatial aliasing become obvious in the form of undesired side lobes.

The presented sound field model assumes that each driver is an ideal point source. At least in the near field of the array, this does not reflect the physical sound field and requires further refinement. The presented simulated beam patterns are solely based on the developed model and still require

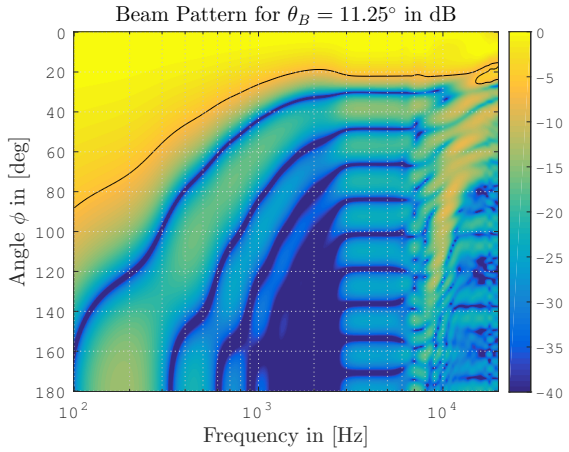

(a) Beam Angle $\theta_B = 11.25°$

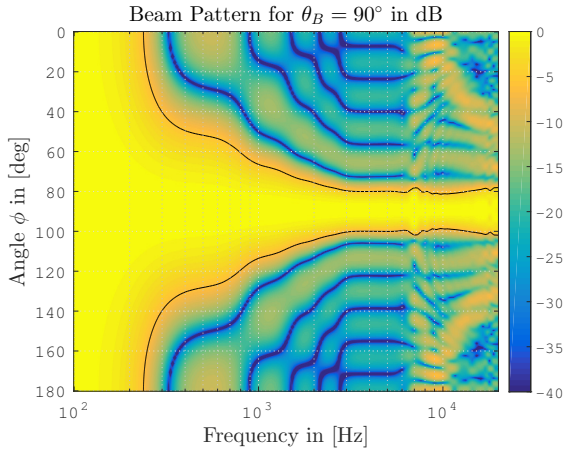

(b) Beam Angle $\theta_B = 90°$

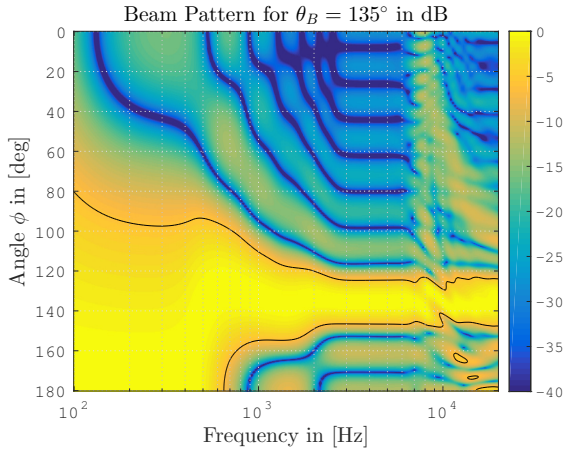

(c) Beam Angle $\theta_B = 135°$

Figure 5: Various normalised beam patterns as a function of frequency for three beam angles.

confirmation through thoroughly conducted measurements.

6 Conclusions

A mathematical model for the radiation from a hemi-cylindrical loudspeaker array on an infinite baffle has been presented. The beamforming method for sound field control has been derived from the solution to the inverse problem. Theoretically achievable beam patterns have been presented for various beam directions as a function of frequency. It was found that the beam pattern changes as a function of the steering angle, which is a consequence of the lack of symmetry combined with the cosine basis functions. On the basis of the simulated beam patterns, an estimate of the optimal frequency band for an array with 15 speakers was given. The overall system performance appears to be comparable to that of cylindrical loudspeaker arrays.

Future work will present measurement results and further refinements to the acoustic model, allowing for the description of the near field to be applied to improve sound field control.

7 Acknowledgements

This work has been partially funded by the *Engineering and Physical Science Research Council*, the *Royal Academy of Engineering* and by *HUAWEI*.

References

[1] Daniel, J., Moreau, S., and Nicol, R., "Further Investigations of High-Order Ambisonics and Wavefield Synthesis for Holophonic Sound Imaging," in *Audio Engineering Society Convention 114*, 2003.

[2] Poletti, M. A., "Three-Dimensional Surround Sound Systems Based on Spherical Harmonics," *Journal of the Audio Engineering Society*, 53(11), pp. 1004–1025, 2005.

[3] Ahrens, J. and Spors, S., "An Analytical Approach to Sound Field Reproduction using Circular and Spherical Loudspeaker Distributions," *Acta Acustica united with Acustica*, 94(6), pp. 988–999, 2008.

[4] Teutsch, H. and Kellermann, W., "Acoustic source detection and localization based on wavefield decomposition using circular microphone arrays," *Journal of the Acoustical Society of America*, 120(5), pp. 2724–2736, 2006.

[5] Fazi, F. M. and Nelson, P. A., "Sound field reproduction using directional loudspeakers and the equivalent acoustic scattering problem," 2010.

[6] Kolundzija, M., Faller, C., and Vetterli, M., "Baffled circular loudspeaker array with broadband high directivity," in *Proceedings of the IEEE International Conference on Acoustics, Speech, and Signal Processing, ICASSP 2010, 14-19 March 2010, Sheraton Dallas Hotel, Dallas, Texas, USA*, pp. 73–76, IEEE, 2010, ISBN 978-1-4244-4296-6, doi:10.1109/ICASSP.2010.5496204.

[7] Kolundzija, M., Faller, C., and Vetterli, M., "Design of a Compact Cylindrical Loudspeaker Array for Spatial Sound Reproduction," in *Audio Engineering Society Convention 130*, Audio Engineering Society, 2011.

[8] Poletti, M. and Betlehem, T., "Design of a Prototype Variable Directivity Loudspeaker for Improved Surround Sound Reproduction in Rooms," in *Audio Engineering Society Conference: 52nd International Conference: Sound Field Control - Engineering and Perception*, 2013.

[9] Betlehem, T. and Poletti, M. A., "Two dimensional sound field reproduction using higher order sources to exploit room reflections," *The Journal of the Acoustical Society of America*, 135(4), pp. 1820–1833, 2014, doi:http://dx.doi.org/10.1121/1.4868376.

[10] Poletti, M. A., Betlehem, T., and Abhayapala, T. D., "Higher-Order Loudspeakers and Active Compensation for Improved 2D Sound Field Reproduction in Rooms," *J. Audio Eng. Soc*, 63(1/2), pp. 31–45, 2015.

[11] Fazi, F. M., Shin, M., Olivieri, F., Fontana, S., and Lang, Y., "Comparison of Pressure-Matching and Mode-Matching Beamforming for Methods for Circular Loudspeaker Arrays," in *Audio Engineering Society Convention 137*, Audio Engineering Society, 2014.

[12] Fazi, F. M., Shin, M., Olivieri, F., and Fontana, S., "Low Frequency Performance of Circular Loudspeaker Arrays," in *Audio Engineering Society Convention 138*, Audio Engineering Society, 2015.

[13] Williams, E. G., *Fourier Acoustic: Sound Radiation and Nearfield Acoustical Holography*, Academic Press, 1999.

[14] Kirszenstein, J., "An Image Source Computer Model for Room Acoustics Analysis and Electroacoustic Simulation," *Applied Acoustics*, 17, pp. 275–290, 1984.

[15] Bronstein, I. N., Semendjajew, K. A., Musiol, G., and Mühlig, H., *Taschenbuch der Mathematik*, Verlag Harri Deutsch, 2006.

[16] Colton, D. and Kress, R., *Inverse Acoustic and Electromagnetic Scattering Theory, Series 93 Applied Mathematical Sciences*, Springer, 1998.

[17] Newell, P. and Holland, K., *Loudspeakers: For Music Recording and Reproduction*, Focal, 2007, ISBN 9780240520148.

[18] Kreyszig, E., *Introductory Functional Analysis with Application*, Wiley, 1978.

[19] Rafaely, B., "Analysis and Design of Spherical Microphone Arrays," *IEEE Transactions on Speech and Audio Processing*, 13(1), pp. 135–143, 2005.

[20] Fazi, F. M., *Sound Field Reproduction*, Ph.D. thesis, University of Southampton, Faculty of Engineering, Science and Mathematics, Institute of Sound and Vibration Research, 2010.

[21] Hoffmann, F.-M. and Fazi, F., "Theoretical Study of Acoustic Circular Arrays With Tangential Pressure Gradient Sensors," *Audio, Speech, and Language Processing, IEEE/ACM Transactions on*, 23(11), pp. 1762–1774, 2015, ISSN 2329-9290, doi:10.1109/TASLP.2015.2449083.

[22] Fazi, F. M. and Nelson, P. A., "The Ill-Conditioning Problem in Sound Field Reconstruction," in *Audio Engineering Society Convention 123*, 2007.